

Servomotor Dataset: Modeling Health in Mechanisms with Typically Intermittent Operation

Arun Subramanian¹, Abhinav Saxena², and Jamie Coble³

^{1,2} *GE Research, Niskayuna, NY, 12309, USA*
arun.subramanian1@ge.com
asaxena@ge.com

³ *University of Tennessee, Knoxville, TN, 37996, USA*
jcoble1@utk.edu

ABSTRACT

Servomotors are used in a variety of industrial applications where precise movements are of critical importance. Degradation mechanisms in servo motors have been mostly studied and modeled for systems with long duration steady state modes. However, some specialized applications require health estimation from very short duration intermittent operations, which require different analysis techniques. With such applications in mind, a simulated dataset for servomotor health modeling and prediction is described and made available for public use. The application scenario is motivated by a fine motion control rod drive (FMCRD) mechanism used for *intermittent*, and typically infrequent, fine motion (insertion or withdrawal) adjustment of control rods in some nuclear reactor designs. Though the drives do not run continuously, servomotor and associated linear motion mechanisms do show wear and damage during its operational lifetime. Specifically, in FMCRD such degradations may be caused by internal as well as external damage to the system. While the causes of such damage can be diverse, in simulation we model the *impact* of cumulative damage as an external opposing load which resists the movement of the motor shaft. Such scenarios represent effects of rod-binding and debris in the fuel channels. The dataset includes measurements such as motor currents and rotor speed which would be part of the instrumentation in a typical deployments of rotating machinery. These observable measurements can be used to predict the health state of the servomotor. Also presented are baseline results on health state estimation, formulated as classification and regression problems, which can be used by the larger PHM community for performance comparisons. This dataset

is hosted at the PHM Society Data repository (Subramanian, Saxena, & Coble, 2023).

1. INTRODUCTION

Servomotors are utilized in a variety of industries for their closed-loop feedback systems that provide high-precision control and accuracy of the rotor's speed and position. The current work is motivated by the use of servomotor drives in some nuclear power plants. In fission reactors, in the context of nuclear power generation, neutron-absorbing control rods are used to modulate the reactivity by precise positioning within the reactor core. While the control rods serve to rapidly shutdown the reactor completely when a safety trigger gets tripped, incremental positioning of the rods, as a part of normal operation, enables optimized power control and core power shaping. The former, also known as a SCRAM, is typically controlled by a hydraulic mechanism. Fine motion control rod drives (FMCRD) are used to operate the control rods for the latter purpose and are driven by electric servomotors. For example, the advanced boiling water reactor (AWBR) by GE Hitachi has a suite of 205 FMCRDs (*Chapter 4: Reactor, AWBR: Design Control Document / Tier 2*, 2016). More recently, small modular reactors (SMR) have become an important consideration in the energy mix for the flexibility and scalability they afford, among other advantages. The BWRX-300 is a SMR proposed by GE Hitachi Nuclear Energy (GE Hitachi Nuclear Energy, 2023, 2020) which has a similar set of control rods arranged in the reactor core, with each being driven by a dedicated FMCRD.

In both the AWBR and the SMR designs, the FMCRD makes small positional adjustments to the control rods and for a power maneuver. This means that the bulk of the servomotor operation happens in small spurts and the motor does not operate for extended durations. This is in contrast to most rotating machinery that operates on a more continuous basis and

Arun Subramanian et al. This is an open-access article distributed under the terms of the Creative Commons Attribution 3.0 United States License, which permits unrestricted use, distribution, and reproduction in any medium, provided the original author and source are credited.

sustains wear over steady state operation (e.g., see (Bejaoui, Bruneo, & Xibilia, 2020)). Although the drive operates over short durations, internal as well as external damage can cause impediments to the movement of the rotor shaft, leading to modes of degradation that differ from continually operating servomotors. The prognostics and health management for such an intermittent operational regime is different, and this paper addresses the need for data and algorithms for such applications. Specifically, for machine learning approaches, feature extraction over periods of transient operation requires different preprocessing and signal analysis than features one may extract over continuously operating machinery.

Specifically, in this paper we present a simulated dataset for a generic servomotor driven ball-screw mechanism inspired by FMCRD use-case. We first describe the simulator design in Section 2. We discuss the design of experiments and describe the data recorded in Section 3 and in Section 4 discuss observations about the data which also explicates the nature of data over various levels of degradation. Section 5 presents baseline results for health prediction.

2. SERVMOTOR SIMULATION

A Mathworks[®] Simulink[®] Simscape based model is used to build a servomotor simulator with coupled ball-screw mechanical components. The motor system is derived from MathWorks’s base three-phase permanent magnet synchronous motor (PMSM) example (The MathWorks, Inc., 2023b, 2023a) and the ball screw system is based on the model used in (Krichen et al., 2020) to simulate a five-axis CNC machine tool.

PMSM are designed to operate at a specific constant speed, in step with the rotating magnetic field. A 220 voltage AC source provides 3-phase sinusoidal voltages to the PMSM. These specific motors use a wound rotor, in which coils of wire are placed in the rotor slots. These coils are excited by an external DC source, slip rings and brushes that are used to supply current to the rotor. The Simulink model diagram is shown in Fig. 1 where the 3-phase motor system (red block) feeds rotor speed and torque data to simulate a force that drives the actuator system (green block). This model demonstrates the implementation for nominal operation, without faults or degradation.

Figure 2 is a simplified schematic representation of the control loop, adapted from Figure 1 in (Fullilove, Santos, Saxena, & Coble, 2022). The degradation mechanism is simulated using a “RESISTIVE LOAD” block which is connected to the load being driven by the actuator. This is apparent when we compare the “green components”, i.e., the actuator block in Fig. 1 with the drive mechanism in Fig. 2. The resistive load represents the force acting against the ball screw. Increasing this load mimics the effect of causes of FMCRD degradation such as friction, debris and rod binding.

At a given instant, a demanded position drives the ball screw via the servomotor. A Matlab wrapper interfaces with the Simulink model to enable setting a desired control rod movement/displacement profile. The desired position is compared to the current position measurement of the encoder and the calculated difference is converted by the PID controller to an input speed that corrects and achieves the desired position. Not shown in Fig. 2, but included within the Simulink model, are 2 PI controllers that ramp rotor speed to its desired value. Finally, the 3-phase motor currents are converted to an orthogonal reference frame (direct and quadrature) using the Parke and Clarke transform. Implementing these two transforms in a consecutive manner simplifies computations by converting AC current and voltage waveform into DC signals. Finally, the output measurements of the model are the stator phase currents, rotor speed, electromagnetic torque, and Q - and D -axis phase currents. An external braking system is also used to apply a force to the motor shaft once the desired position is obtained, locking the control rod in place. While the PID controller in its nominal operation is tuned to be a critically damped system, adding the resistive load block changes the control profile. We also add band-limited measurement noise into the feedback loop which further moves the output response to be under-damped under certain realizations of noise and resistive load. Thus the simulator is not an idealized notion of servo control, but indeed incorporates real-world operational conditions.

3. DATASET DESCRIPTION

In previous work, (Fullilove et al., 2022) have described methods for fault detection, with different fault modes added to the Simulink model described shown in Fig. 1. For this work, the simulator is exercised for generating representative data in the presence of resistive load that acts against the servomotor ball screw mechanism. This section describes the design of experiments and the resulting dataset.

Data are simulated as depicted in Fig. 3. We consider 4 categories of load values denoted as $\mathbb{C} \triangleq \{c = 0, 1, 2, 3\}$. These map one-to-one with 4 levels of degradation $\{\text{'LN'}, \text{'LO'}, \text{'MED'}, \text{'HI'}\}$ which denote the labels like-new, low, medium and high, respectively. The load is a latent unobservable variable, but its effects may be manifested in observable signals from the Simulink model. The loads are sampled from a mixture of Gaussians with distinct modes corresponding to each category c . Consequently, each measurement from the simulation maps to a degradation level ($DL \in \{\text{'LN'}, \text{'LO'}, \text{'MED'}, \text{'HI'}\}$) and a *degradation value*, $DV \in \mathbb{R}^+$. Each DV is normally distributed with mean μ_{DL} and standard deviation σ_{DL} . We assume that as part of existing inspection protocols, subject matter experts, SMEs, have a way of determining DV and DL . For this dataset, DV is not upper-bounded, though a user may use suitable monotone functional transforms so that, e.g., $DV \in [0, 1)$.

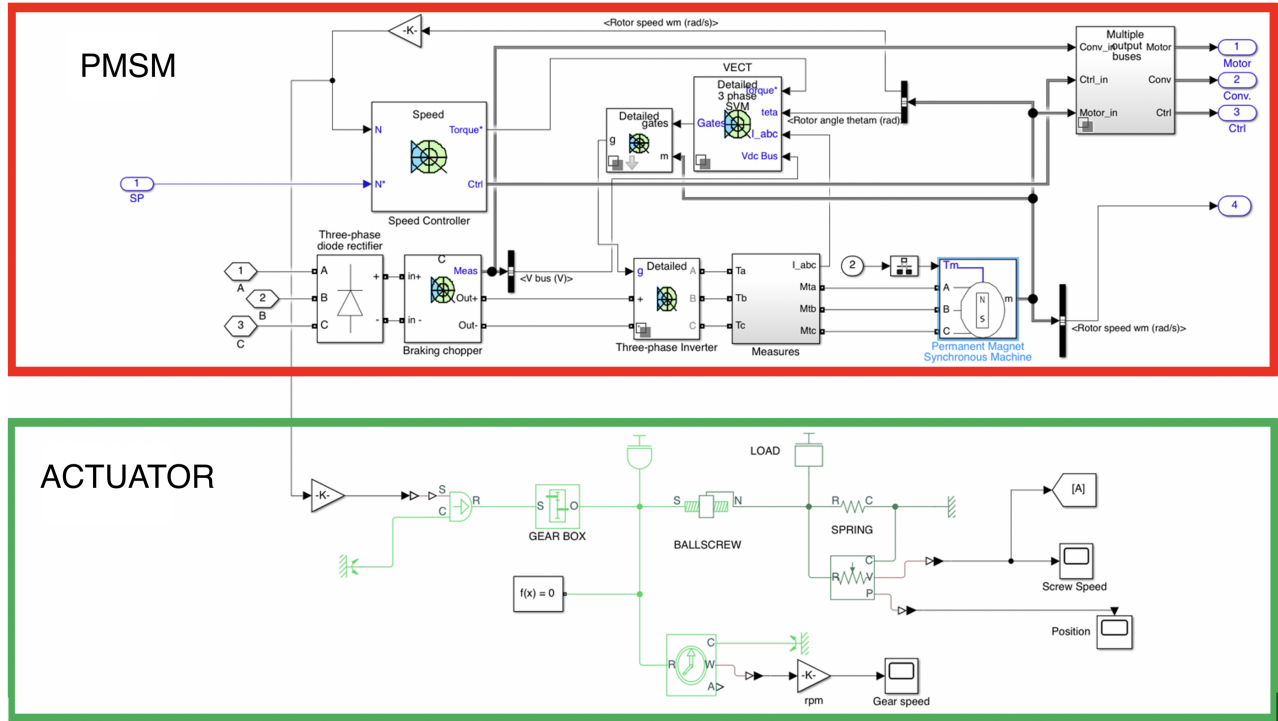


Figure 1. Simulink/SimScape model for the servomotor simulation: PMSM and actuator

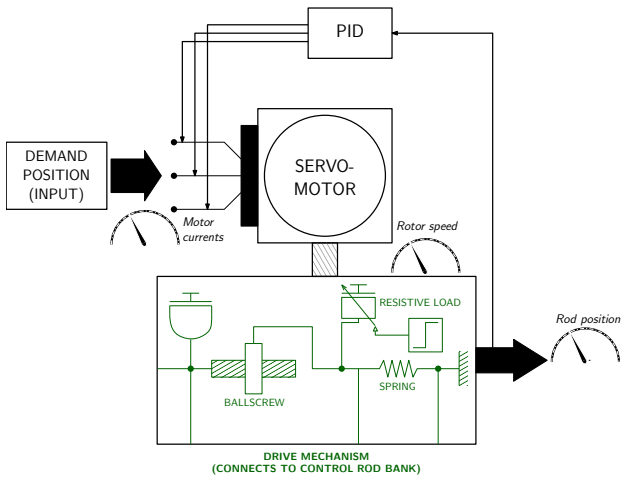


Figure 2. Simulink/SimScape model for the servomotor simulation: Simplified schematic showing control loop and fault injection. Adapted from (Fullilove et al., 2022).

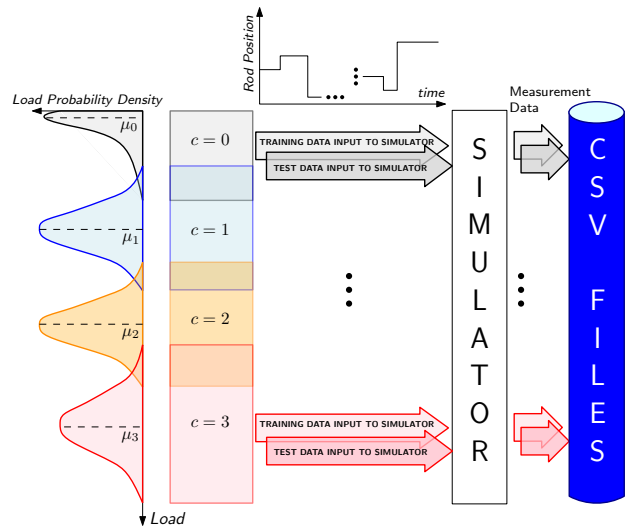


Figure 3. Data generation methodology.

Table 1 lists the values of μ_{DL} , σ_{DL} . As evident by the histogram in Fig. 4, there is an overlap of DV between adjacent degradation levels. This also mimics the ambiguity in assessments by SMEs about what may constitute a medium vs. high level of degradation.

In exercising the simulator, we also input a randomly generated sequence of demanded rod positions (equivalently rod displacements); every such sequence is called a *run*. A rod

displacement is referred to as a *transition* in that the rod transitions from a previous position to a new demanded position. For each FMCRD degradation category, we generate 200 distinct runs, which consists of an initial rod position and a sequence of 5 transitions (demanded displacements) of the control rod over a period of 6 seconds. This is simply an accelerated mechanism to simulate an ensemble of typical displacements of the control rod. A run of transitions, however, may not necessarily be a typical sequence of what is com-

Table 1. Simulation parameters for load categories.

	Degradation Level, DL			
	'LN'	'LO'	'MED'	'HI'
Mean, μ_{DL}	0	400	1600	3200
Standard deviation, σ_{DL}	2	200	300	500

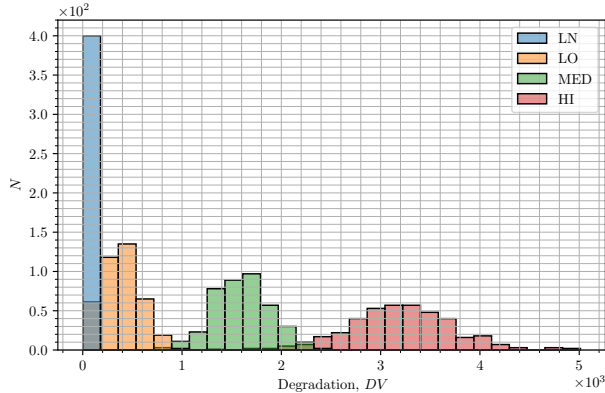


Figure 4. Histogram of load values.

manded over a 6s duration. This is schematically represented in Fig. 3. The blocks labeled $c = 0$ to $c = 3$, next to the Load Probability Densities, represent the 200 loads sampled for each c , and the rod position vs. time graph represents a run generated as the input to the simulator. The rod displacements are sampled uniformly from $(-20, -4) \cup (4, 20)$ mm. Exercising the simulator in this way, we obtain a dataset of FMCRD measurements corresponding to 1000 transitions for each degradation category. Note that all transitions corresponding to a given run have the same degradation value; however, two distinct runs will have distinct DVs .

Each transition is characterized by several measurements over time since the data are simulated over a sampling rate of 50 kHz. The recorded data include the timestamp, demanded rod position, actual rod position, rotor speed, servo motor stator currents (Phase A/B/C as well as the direct and quadrature transforms) and torque. As stated earlier, we include a categorical degradation label from {'LN', 'LO', 'MED', 'HI'} as well as a floating point degradation value.

The simulator is exercised twice with different seeding of the random number generators for training data and test data respectively; this is represented by the block arrows in Fig. 3. For each dataset, training and testing, the full data table consists of 240 million rows ($50 \text{ kHz} \times 6\text{s} \times 200 \text{ runs per } DL \text{ type} \times 4 \text{ } DL \text{ types}$). The data are stored as CSV files. Table 2 provides a description the various columns in the dataset. The data are hosted at the PHM Society Data Repository (Subramanian et al., 2023).

The panel of 6 plots at the bottom of Fig. 5 shows the degra-

Table 2. Dataset variables.

Column name	Description
time	Timestamp for each run
DV	Degradation value
rod_demand_pos	Demanded rod position
rod_actual_pos	Actual rod position
torque	Motor torque
rotor_speed	Rotor speed
i_3p_a	Stator current: Phase A
i_3p_b	Stator current: Phase B
i_3p_c	Stator current: Phase C
direct	Direct component of DQZ transform on the stator currents
quadrature	Quadrature component of DQZ transform
run_index	Index of runs
transitions	Index of transitions
del_pos	Demanded displacement, i.e., position delta
ylabel	Categorical degradation levels; $ylabel \in \{"LN", "LO", "MED", "HI"\}$

dation values, and demanded and actual displacements, for pairs of consecutive runs sampled from different low, medium and high degradation levels. As one can observe, each run consists of transitions corresponding to positive or negative displacements of the control rod. In the dataset, runs are indexed by `run_index`, and transitions are indexed by the column labeled `transitions`. While the `run_index` values in each subplot are consecutive, this does not imply that it is a function of usage or life since the runs are random draws from the underlying sampling distributions. Temporal information indicating life or usage history is not explicitly modeled. In fact, two closely spaced degradation values, as sampled from the degradation profile in the top panel of Fig. 5, may be separated by a considerable gap in time. It is also important to note that since runs are simulated as IID samples from an underlying distribution, 2 successive runs may be considered to be realizations from an *ensemble* of similar control rods and drives. This also mimics what is typical: deployment as bank of a control rods and drives. One may apply various damage propagation models such as those considered by (Saxena, Goebel, Simon, & Eklund, 2008) or (Liang et al., 2014) to simulate time-to-failure data, but this is not within the scope of our approach.

4. DATASET ANALYSIS

Time-series snapshots of the collected dataset are shown in the Appendix (Fig. 9) as a full-page plot for ease of reference. The rod position panel plots both the demanded (green) as

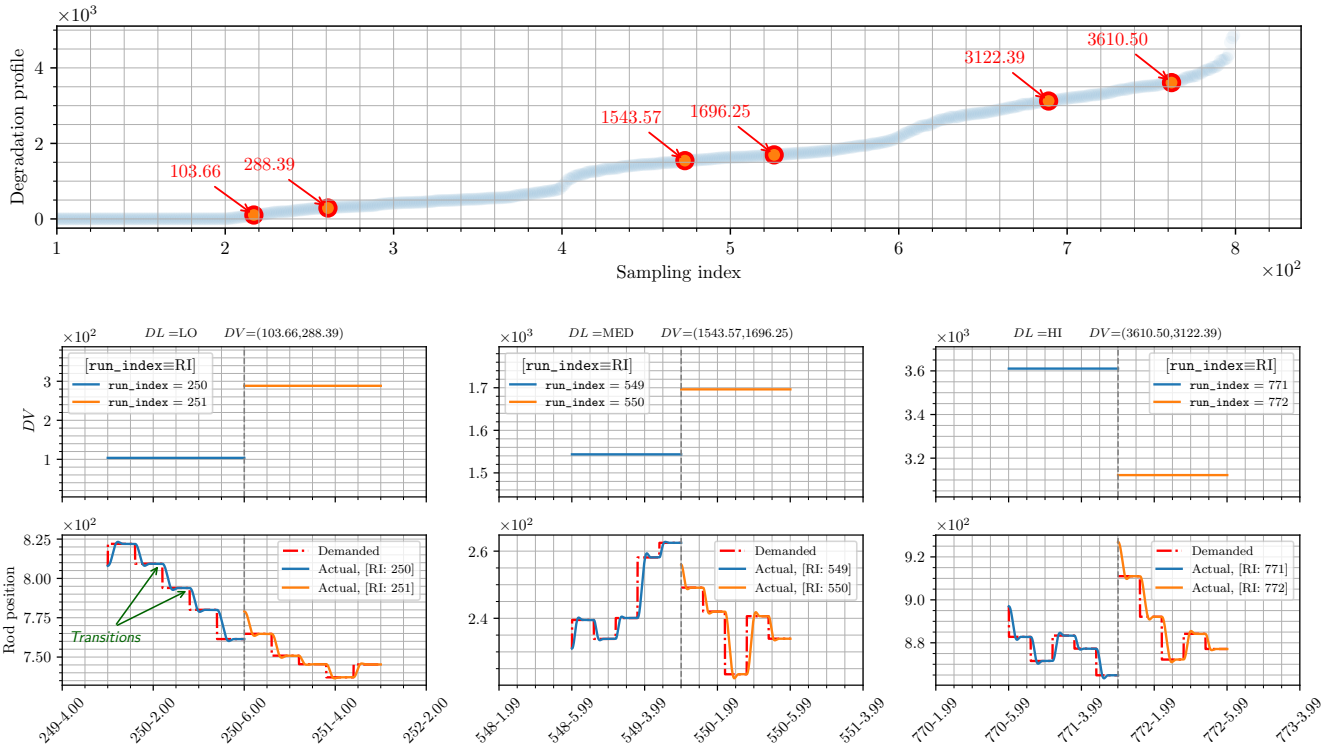


Figure 5. Runs and transitions for different loads. Note that all transitions corresponding to a given run have the same degradation value; however, two distinct runs will have distinct DVs.

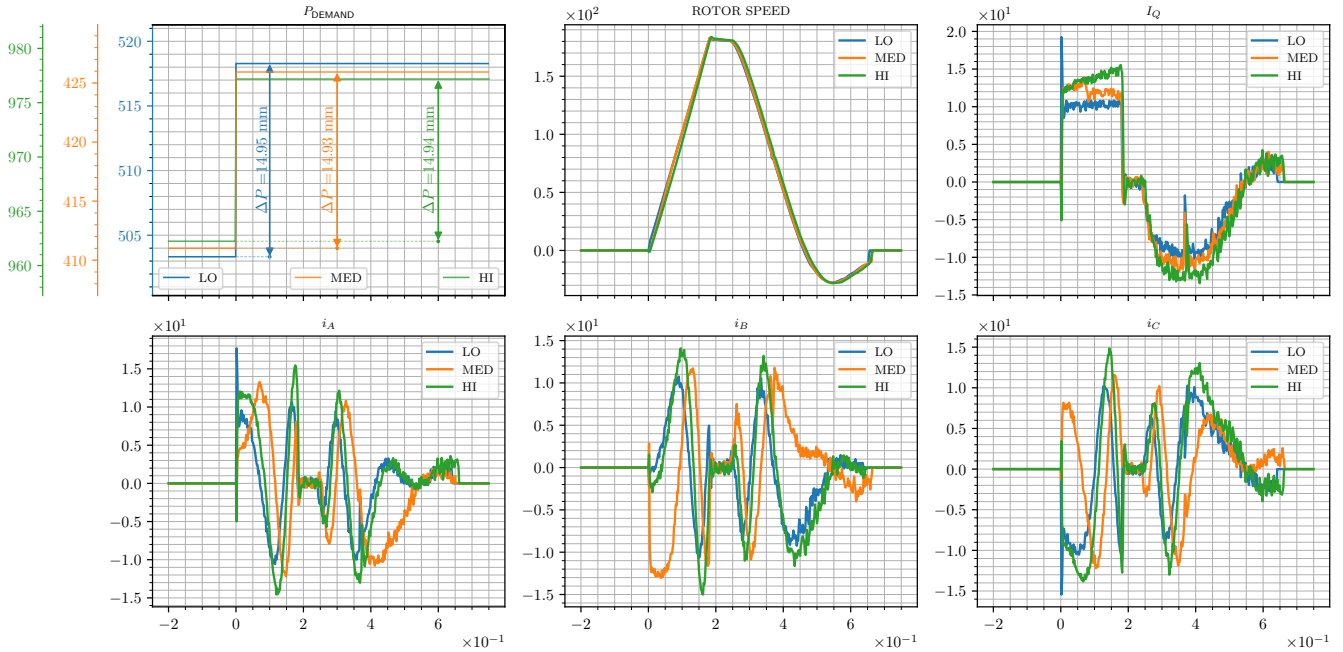


Figure 6. Measured variables over a similar displacement across different degradation levels.

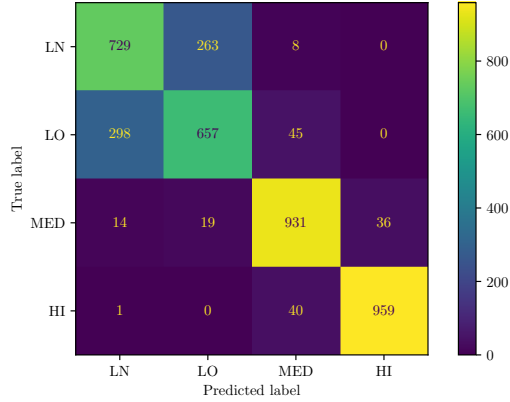


Figure 7. Confusion matrix.

well as actual rod positions. In all panels, the red markers are data representing the portion of acquired signals during which the rotor shaft is in motion.

Degradation signatures are visible in the time-series data for segments corresponding to intervals when the motor is in operation. E.g., examining the stator AC currents and their quadrature component shows a separation for different load levels. In Fig. 6, the demanded displacement is within comparable magnitude for 3 different degradation levels (displacement of 14.93 ± 0.01 mm for exemplar transitions from LO, MED and HI cases, respectively). The timestamps have been adjusted to start at 0. This suggests that data-driven health state prediction is possible.

5. HEALTH MODELING AND PREDICTION

In this section, the dataset is used for modeling and predicting the health state of the FMCRD. Two setups are considered:

- Classification, where y_{label} is used as a target;
- Regression, where real valued DV is the target

Simple features are used to setup baseline results. Recall that in the context of the problems being considered, only segments of time-series data while the rod is in motion (transient data) is useful. We first segment the transient portion of the data - this is easily extracted by allowing for a tolerance of convergence between the demanded and actual rod position, as well as using a persistent return-to-zero logic in signals such as rotor speed or torque. For each transition, a transient segment is split into 3 equal time intervals and median values for rotor speed and quadrature current are computed over each interval. Including del_pos , we get a 7-dimensional feature vector.

To solve the classification problem, we train a random forest classifier, the results for which are presented in Fig. 7 and Table 3. Using the same feature set, we also train with DV as the response variable using a random forest and a support vector regressor (SVR) with a radial basis kernel. The scatter

Table 3. Classification metrics

	LN	LO	MED	HI
Precision	0.96	0.70	0.91	0.70
Recall	0.96	0.66	0.93	0.73
F_1 score	0.96	0.68	0.92	0.71
N	1000	1000	1000	1000
Accuracy	0.82			

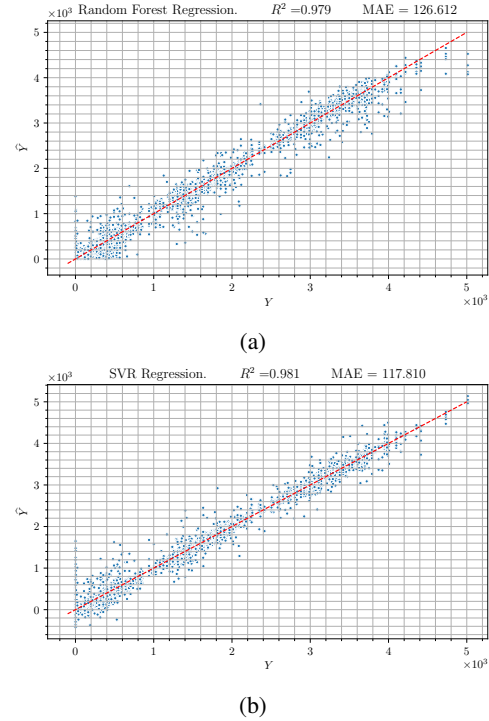


Figure 8. Scatter plot of \hat{Y} vs. Y for health state estimation as a regression problem using (a) random forest regressor and (b) a support vector regressor.

plots of predicted vs. actual (\hat{Y} vs. Y) is presented in Fig. 8a and Fig. 8b. While the SVR model achieves a lower mean absolute error (MAE) compared to the random forest regressor, the forest of decision rules is able to learn a decision region that excludes $DV < 0$. This likely has implications for generalizability when the model encounters data in regimes where it has not seen training data.

6. CONCLUSION

We described a simulated dataset for fine motion motion control rod drives, which are operated intermittently and age as a function of transient usage. The datasets are designed for machine learning approaches to model and degradation: we have generated training and testing sets, with measurement data that is typically available during deployment, and data

labels which may be treated as SME evaluations. This paper also discusses baseline results which can be used for performance comparisons. We encourage users to consider ways in which the data can be used for health prediction, prognostics and decision aiding by using better algorithms or imposing different constraints. As part of current and future work we are also evaluating the suitability of releasing the Simulink model and simulation scripts for public use.

ACKNOWLEDGMENT

Authors would like to acknowledge GE Hitachi's support in providing guidance and cost share. The information, data, or work presented herein was funded in part by the Advanced Research Projects Agency-Energy (ARPA-E), U.S. Department of Energy, under Award Number DE-AR0001290. The views and opinions of authors expressed herein do not necessarily state or reflect those of the United States Government or any agency thereof.

REFERENCES

- Bejaoui, I., Bruneo, D., & Xibilia, M. G. (2020). A data-driven prognostics technique and rul prediction of rotating machines using an exponential degradation model. In *2020 7th International Conference on Control, Decision and Information Technologies (CoDIT)* (Vol. 1, p. 703-708). doi: 10.1109/CoDIT49905.2020.9263930
- Chapter 4: Reactor, AWBR: Design Control Document / Tier 2 (Vol. 25A5675AF Revision 6). (2016, February). GE Hitachi Nuclear Energy. Retrieved June 8, 2023, from <https://www.nrc.gov/docs/ML1608/ML16081A093.pdf>
- Fullilove, N., Santos, D. D., Saxena, A., & Coble, J. (2022, Oct). Leveraging within-bank comparison for anomaly detection, diagnostics, and prognostics in advanced nuclear power plants. *Annual Conference of the PHM Society*, 14(1). doi: 10.36001/phmconf.2022.v14i1.3215
- GE Hitachi Nuclear Energy. (2020). *BWRX-300 Fact Sheet*. Retrieved June 13, 2023, from https://nuclear.gepower.com/content/dam/gepower-nuclear/global/en_US/documents/product-fact-sheets/BWRX-300_Fact_Sheet-2020.pdf
- GE Hitachi Nuclear Energy. (2023). *BWRX-300*. Retrieved June 13, 2023, from <https://nuclear.gepower.com/build-a-plant/products/nuclear-power-plants-overview/bwrx-300>
- Krichen, M., Elbouchikhi, E., Benhadj, N., Chaieb, M., Benbouzid, M., & Neji, R. (2020, June). Motor Current Signature Analysis-Based Permanent Magnet Synchronous Motor Demagnetization Characterization and Detection. *Machines*, 8(3), 35. doi: 10.3390/machines8030035
- Liang, S. Y., Li, Y., Billington, S. A., Zhang, C., Shiroishi, J., Kurfess, T. R., & Danyluk, S. (2014). Adaptive prognostics for rotary machineries. *Procedia Engineering*, 86, 852-857. (Structural Integrity) doi: 10.1016/j.proeng.2014.11.106
- Saxena, A., Goebel, K., Simon, D., & Eklund, N. (2008). Damage propagation modeling for aircraft engine run-to-failure simulation. In *2008 international conference on prognostics and health management* (p. 1-9). doi: 10.1109/PHM.2008.4711414
- Subramanian, A., Saxena, A., & Coble, J. (2023). *Servomotor Driven Ballscrew Mechanism Data Set*. Retrieved June 13, 2023, from https://data.phmsociety.org/servomotor_dataset/
- The MathWorks, Inc. (2023a, June). *AC6 - PM Synchronous 3HP Motor Drive*. Retrieved June 9, 2023, from <https://www.mathworks.com/help/sps/ug/ac6-pm-synchronous-3hp-motor-drive.html>
- The MathWorks, Inc. (2023b, June). *PM Synchronous Motor Drive: Implement Permanent Magnet Synchronous Motor (PMSM) vector control drive*. Retrieved June 9, 2023, from <https://www.mathworks.com/help/sps/powersys/ref/pmsynchronousmotordrive.html>

APPENDIX

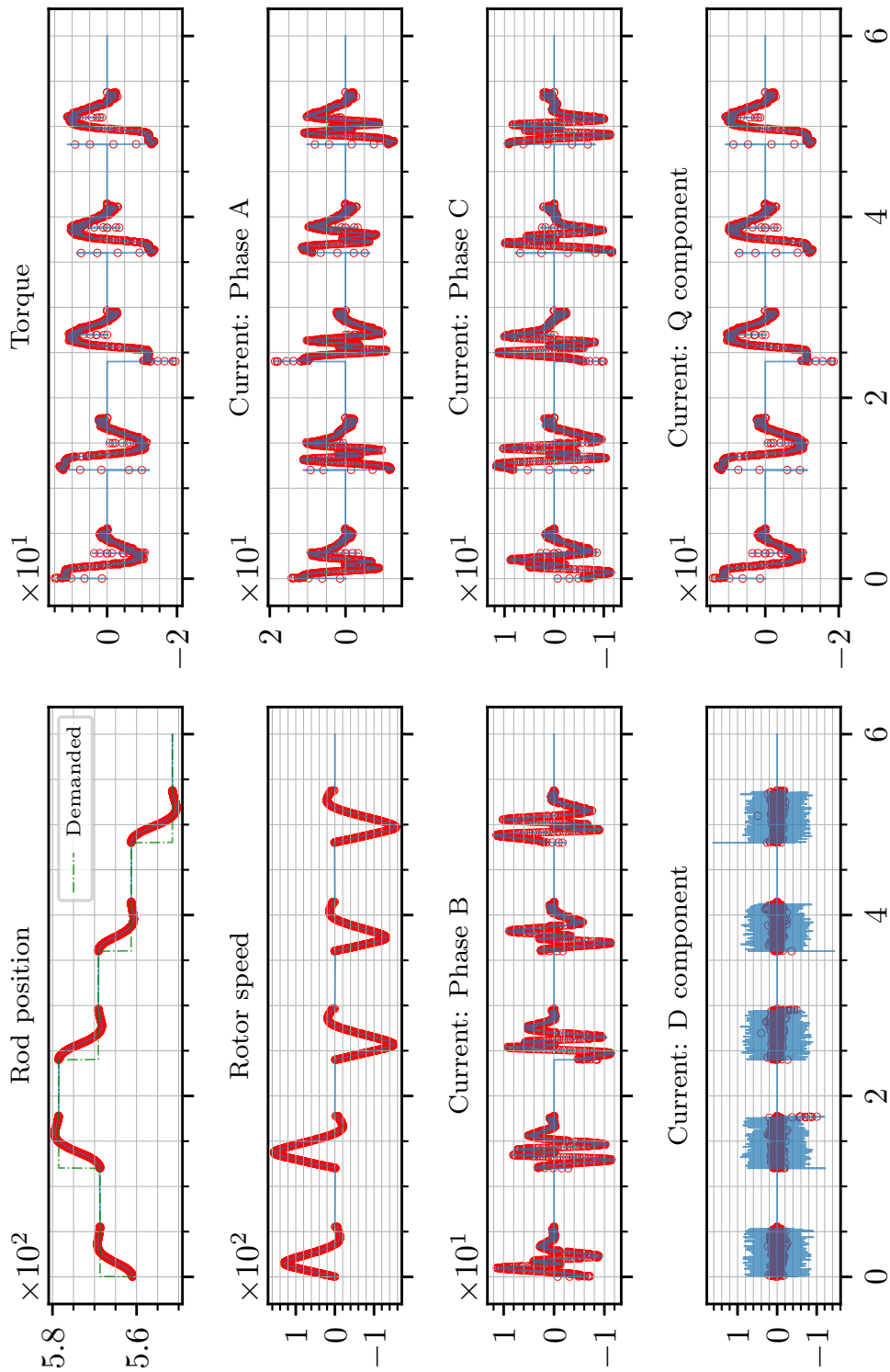


Figure 9. Example of a time-series plot for a run.